



ELSEVIER

Available online at www.sciencedirect.com

SCIENCE @ DIRECT®

Solar Energy Materials
& Solar Cells

Solar Energy Materials & Solar Cells 80 (2003) 105–113

www.elsevier.com/locate/solmat

Modeling the optical absorption within conjugated polymer/fullerene-based bulk-heterojunction organic solar cells

H. Hoppe^{a,*}, N. Arnold^b, N.S. Sariciftci^a, D. Meissner^{a,c}

^aLinz Institute for Organic Solar Cells (LIOS), Johannes Kepler University, Altenbergerstr. 69, Linz A-4040, Austria

^bAngewandte Physik, Johannes Kepler University, Altenbergerstr. 69, Linz A-4040, Austria

^cUniversity of Applied Sciences, Roseggerstr. 12, Wels A-4600, Austria

Received 7 October 2002; accepted 15 April 2003

Abstract

In this paper, we report our results on the modeling of the optical properties of the bulk-heterojunction “plastic solar cells”, consisting of a solid-state blend of the conjugated polymer poly-[2-(3,7-dimethyloxy)-5-methoxy]-para-phenylene-vinylene and the fullerene C₆₀ derivative 1-(3-methoxycarbonyl) propyl-1-phenyl [6,6]C₆₁. Upon illuminating these cells with the standard AM 1.5 solar spectrum, the short circuit current can be determined for any given internal quantum efficiency as a function of the active layer thickness. In addition, the depth profiles of photoinduced charge generation rates are calculated. Based on the agreement of this modeling with experimentally determined efficiencies of these solar cells, an internal quantum efficiency of about 80% has been estimated.

© 2003 Elsevier B.V. All rights reserved.

Keywords: Optical modeling; Plastic solar cell; Absorption; Refractive index; Internal quantum efficiency

1. Introduction

In order to gain a better understanding of the limiting factors for the efficiency of the polymer/fullerene bulk-heterojunction-based “plastic solar cell” [1–2], the actual absorption profile within the photoactive layer of this multilayer device is of

*Corresponding author.

E-mail address: harald.hoppe@jku.at (H. Hoppe).

fundamental interest. The photoactive layer consists of an interpenetrating network of poly-[2-(3,7-dimethyloctyloxy)-5-methyloxy]-para-phenylene-vinylene (MDMO-PPV) and 1-(3-methoxycarbonyl) propyl-1-phenyl [6,6]C₆₁ (PCBM) with a mixing ratio of usually 1:4 by weight. At the interface between these materials, a fast electron transfer from the MDMO-PPV to PCBM takes place upon light excitation [2,3]. Then the respective charge carriers (electrons and holes) are transported within the two separate materials to the electrical contacts of the solar cell. The performance of these plastic solar cells based on bulk heterojunctions between the conjugated polymer donors and fullerene-type acceptors has been reported to be up to 2.5% at AM 1.5 white light illumination [2]. From reflection measurements, it is known [2] that for an active layer thickness of about 100 nm used in these devices, the absorption was estimated to be less than 60% of the incoming light at 460 nm. Therefore, an increase of the absorption is required to increase the efficiency of the cells. As the incident photon to collected electron efficiency of this device was measured to be around 50%, an internal quantum efficiency (absorbed photon to collected electron efficiency) of about 85% was estimated.

Hence, there is still some potential left for more absorption and thereby a higher efficiency even without a change of the spectral distribution of the absorption. Thus the question of an optimized active layer thickness shall be addressed in this paper. Optical modeling of absorption and photocurrent spectra has already been performed previously on some (small-molecule) bi-layer heterojunction solar cell systems. Here the critical issue has been found at placing the electric field maximum of the light at the interface of the donor and acceptor layers, since only there the charges are separated in these bilayer junctions [4–7].

Optical modeling has also been performed on classical solid-state semiconductor solar cells and modules where angular-dependent light trapping by multiple internal reflections through surface texturing often has to be taken into account [8–15]. Other papers report on these effects in dye-sensitized nanocrystalline solar cells [16]. Recently, the potential for light trapping in bulk-heterojunction organic solar cells has been numerically investigated for soft embossed diffraction gratings [17].

We present the results of optical modeling of our whole device by using the transfer matrix formalism (see e.g. Refs. [18–20]), which is based on the Fresnel formulas for the several interfaces occurring in the device. The results of the optical modeling are compared with existing experimental data and show good agreement for the observed photocurrent.

2. Experiment

MDMO-PPV was provided by Covion (Germany), PEDOT:PSS (poly[3,4-(ethylenedioxy) thiophene]: poly(styrene sulfonate)) (Baytron) by Bayer (Germany) and PCBM was purchased from J.C. Hummelen (University of Groningen, The Netherlands). Films were prepared by spin coating from chlorobenzene solutions of 1:4 (by weight) blends of MDMO-PPV and PCBM as used in our standard plastic solar cells [1–2]. PEDOT:PSS was spin cast from an aqueous solution with a

concentration of 0.5% by weight. As a substrate, fused silica cleaned with isopropanol in an ultrasonic bath previous to spin coating was used. In order to determine the optical constants of both layers of the indium tin oxide (ITO) glass (MERCK, Germany), the transparent ITO was first etched away completely in a mixture of conc. HNO_3 , conc. HCl and distilled H_2O in a ratio of 1:9:10 by volume to allow for the determination of the optical properties of the substrate glass alone. Then the complete ITO glass was measured. Near-normal incidence (7°) transmission and reflection spectra of the spin cast films on fused silica and of the substrates were recorded using a Cary 3G spectrophotometer (Varian, Inc., Palo Alto, USA) in the range between 300 and 900 nm. Organic layer thicknesses have been verified using a tapping mode AFM (Dimension 3100, Digital Instruments, Santa Barbara, USA), by measuring the depths of scratches in the film. The fitting of complex model dielectric functions $\tilde{\epsilon} = \epsilon' + i\epsilon''$ to the transmission and reflection spectra as well as the determination of the active layer thickness from reflection measurements of a complete solar cell was performed using the software SCOUT2 (M. Theiss, Aachen, Germany). The model dielectric functions consist of a constant dielectric background contributing to the real part of the dielectric function, and of so-called Kim oscillators [21], which describe the optical absorption for the electronic transitions. A Kim oscillator allows a continuous shift of the line shape between a Gaussian and a Lorentzian profile. Once the dielectric functions are obtained, the complex refractive index $\tilde{n} = n + ik$ is calculated easily from the correspondence of the dielectric function and the optical constants given by: $\epsilon' = n^2 - k^2$ and $\epsilon'' = 2nk$.

3. Modeling

To model the optical properties of our multilayer system, the so-called Transfer Matrix Formalism is applied [18–20]. Here the multilayer is treated as a one-dimensional system in which the amplitude of the electromagnetic field vector is calculated coherently. Since the electric and the magnetic fields are connected by the Maxwell equations, it is sufficient to calculate only the electric field component. This formalism considers two electromagnetic waves, one propagating in positive direction perpendicular to the interfaces of the multilayer system, and one in the opposite direction. By traveling from layer A to layer B, the wave undergoes Fresnel reflection and transmission, while within a layer the propagation leads to some phase shift of the wave and decay according to the absorption of the material. All, the reflection, the transmission, the phase shift and the absorption can be described in terms of the optical constants n and k . The change of phase and amplitude can thus be written as a 2×2 matrix, treating both, the forward and backward propagation direction. By multiplying these matrices, the change of the electromagnetic field is obtained for a sequence of layers. Thus the amplitude and phase are known within the system at any arbitrary point, and by applying the continuity equation for the energy:

$$Q + \text{div } \vec{S} = 0, \quad (1)$$

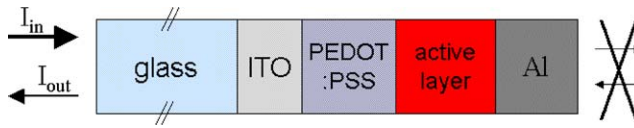


Fig. 1. Schematic structure of the modeled multilayer device. The incoming light (I_{in}) enters the device and propagates attenuated towards the aluminum electrode. There it is reflected and the outgoing intensity (I_{out}) leaves the device through the glass. Due to the high reflectivity and absorption of the aluminum electrode, no light leaves or enters from the right side of the device.

$$\text{with } Q = \frac{1}{2}\omega\epsilon''\epsilon_0 EE^* \quad \text{and} \quad \vec{S} = \frac{1}{2}\text{Re}[E \times H^*],$$

the local absorption within a certain layer can be calculated. Here, ω is the angular frequency of the electromagnetic field, ϵ_0 is the electric permittivity of free space, E the local (depth-dependent) electric field amplitude, Q and \vec{S} denote the local time-averaged absorption and Poynting vector (compare Ref. [22]). While the Poynting vector denotes the electromagnetic energy flux density, its divergence balances the optical absorption that is described by the first term. Eq. (1) is valid for non-magnetic materials in the stationary case.

The program was written using “Mathematica” (WOLFRAM Research, Champaign, IL, USA) and treats the case of normal incidence of the light. The optical modeling has been performed for a cell structure as described before [2], where the light enters through the glass slab, sequentially passing the ITO, the PEDOT:PSS, and the MDMO-PPV:PCBM blend layer. Then the light is reflected back from the Al electrode and finally leaves the solar cell partly at the front again (see Fig. 1). The coherence length of the sunlight is about 800 nm [23]. Thus, in contrast to the thin layers, the much thicker glass slab (thickness d) was treated incoherently. Multiple passes through the glass determine the summated intensity transferred to the glass/ITO interface, calculated as

$$I_{\text{glassITO}} = I_{in} \frac{(1 - R_{\text{airglass}})e^{-\alpha d}}{1 - R_{\text{airglass}}R_{\text{cell}}e^{-2\alpha d}}, \quad (2)$$

where I_{glassITO} is the light intensity in the glass before the glass–ITO interface, R_{airglass} is the reflectivity of the air–glass interface, α is the absorption coefficient of the glass and R_{cell} denotes the total reflectivity of the glass–multilayer interface calculated on the basis of the coherent matrix formalism.

4. Results and discussion

In order to model the optical behavior of the solar cell, all optical constants of the involved layers have been determined previously as described above and published recently [24]. The absorption coefficients $\alpha \equiv 4\pi k/\lambda$, of the polymer, of the fullerene, and of their mixture are shown in Fig. 2 (λ is the wavelength of the light). Both materials, MDMO-PPV and PCBM, contribute to the absorption within the blend. Under standard AM 1.5 solar spectrum irradiation, the contribution of the PCBM to

the absorption within the blend film (about 57%) is even higher than that of MDMO-PPV. This was calculated by simply integrating the standard AM 1.5 solar spectrum multiplied with the respective absorption coefficients of the two materials.

Using Eq. (1), the absorption of light for each wavelength can be calculated for any depth. Thereby it becomes possible to plot the dimensionless differential intensity loss $Q \Delta z / I_{in}$ (per depth $\Delta z = 1$ nm) within the active layer, as shown in Fig. 3 for a 100 nm thick layer. For the five different optical wavelengths shown here the intensity loss varies by about 2–3 orders of magnitude, according to the differences in the electric field and in their optical absorption. Summation over all wavelengths yields the charge generation rate profil. Results for four different

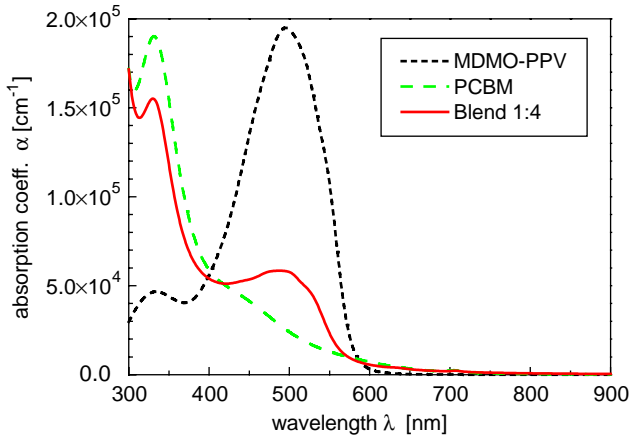


Fig. 2. Absorption coefficients of MDMO-PPV (dotted), PCBM (dashed) and the MDMO-PPV:PCBM 1:4 blend (solid line), calculated from their respective dielectric functions.

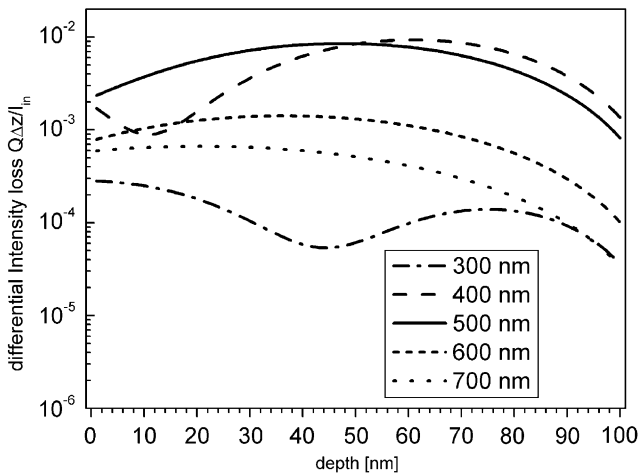


Fig. 3. Fraction of intensity, which is absorbed within 1 nm at a certain depth for several wavelengths, depicted for an active layer thickness of 100 nm. The quantity is normalized to the incident light intensity.

photoactive layer thicknesses are presented in Fig. 4, assuming an incident AM 1.5 standard solar spectrum. The thicker the active layer, the lower the average charge generation rate becomes, while the number of maxima and minima within the profile increases.

The total absorption within the active layer of the solar cell has been calculated as discussed above and its spectral dependence is shown in Fig. 5 for a set of different

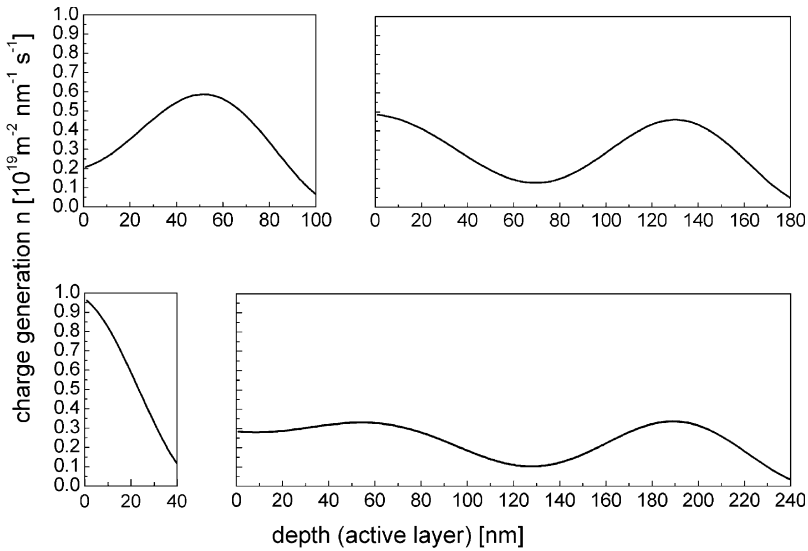


Fig. 4. Charge generation rate profiles for four different thicknesses of the photoactive layer. The thicker the layer, the wavier but also the weaker is the mean charge generation profile.

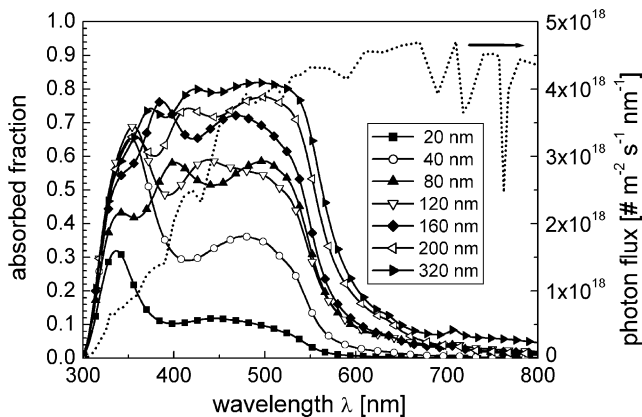


Fig. 5. Fraction of absorbed incident light within the MDMO-PPV:PCBM layer of the solar cell for several layer thicknesses. For comparison, the photon flux of a standard AM 1.5 solar spectrum is shown as a dotted line (right axis). The PEDOT layer thickness is set to 150 nm.

layer thicknesses. For comparison, the photon flux of an AM 1.5 standard solar spectrum is shown as a dotted line. Interestingly due to interference effects, the 120 nm thick film shows no better spectral match with the AM 1.5 standard solar spectrum than the 80 nm thick active layer. Limitations in the precision of the calculated absorption can be a result of slight changes of the optical constants for different film thicknesses. Experimentally, we found some deviations in the absorption coefficients, mainly caused by slightly changing mixing ratios of the polymer and the fullerene in the respective solutions. Here all calculations are based on the optical constants determined for an about 110 nm thick blend film. Assuming an internal quantum efficiency of unity (i.e. no recombination losses within the solar cell), the expected short circuit current under AM 1.5 illumination for different layer thicknesses is depicted in Fig. 6. Interestingly, the short circuit current does not follow a straight line, but shows a local maximum at about 90 nm active layer thickness followed by a plateau until 130 nm. This is also visible in Fig. 5 by the detailed curvature of the spectra from the 80 and 120 nm thick active layer devices. A second increase is located between 140 and 200 nm, followed by another flat region up to 250 nm. Assuming a realistic open circuit voltage of about 0.8 V and a fill factor of 0.6 for an active layer thickness of 100 nm, white light conversion efficiencies of 3% can be calculated from these data under standard AM 1.5 illumination for an internal quantum efficiency of 1. These results are in good agreement with measurements on plastic solar cells [2] where the active layer thickness was estimated to be about 100 nm. This suggests internal quantum efficiencies of about 80% for the bulk-heterojunction “plastic solar cells” based on MDMO-PPV and PCBM. Above 200 nm active layer thickness—assuming again an internal quantum efficiency of 80%—there is a potential for white light conversion efficiencies of about 3.5%.

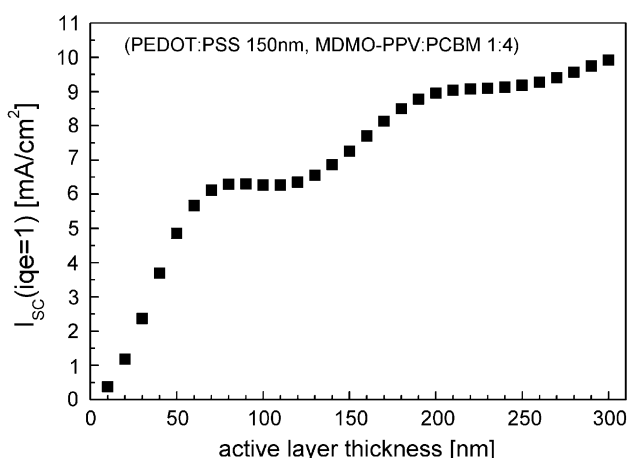


Fig. 6. Calculated short circuit current for different (MDMO-PPV:PCBM 1:4) active layer thicknesses assuming an internal quantum efficiency of unity. The PEDOT layer thickness is set to 150 nm.

5. Conclusions

Optical modeling is an important tool to understand the behavior of solar cell devices consisting of multilayer structures. It was shown that the dependence of the absorption profile within the active layer is not a trivial function of its thickness, but follows—due to interference effects—a rather complicated behavior. In addition, optical modeling provides a rather easy way to optimize the layer thickness of a multilayer device for effective optical absorption. From these data, the photocurrent obtainable from such devices can be calculated for any given incident light spectrum. The results obtained here are in good agreement with experimental results and suggest internal quantum efficiencies of about 80%. The knowledge of the charge generation rates at all depths opens up the possibility for an improved electronic modeling of these devices in the future.

Acknowledgements

Our research was supported by the BMBF-project “Erneuerbare Energien: Organische Solarzellen” (contract number 01SF0026) (Germany). Part of this work was performed within the Christian Doppler Society’s dedicated laboratory on Plastic Solar Cells funded by the Austrian Ministry of Economic Affairs and Quantum Solar Energy Linz GmbH. NA would like to thank FWF project P14700-TPH of the Austrian “Fonds zur Förderung der wissenschaftlichen Forschung” for financial support. DM gratefully acknowledges a fellowship of the Hanse Wissenschaftskolleg, Delmenhorst.

References

- [1] C.J. Brabec, N.S. Sariciftci, J.C. Hummelen, *Adv. Funct. Mater.* 11 (2001) 15.
- [2] S.E. Shaheen, C.J. Brabec, N.S. Sariciftci, F. Padinger, T. Fromherz, J.C. Hummelen, *Appl. Phys. Lett.* 78 (2001) 841.
- [3] N.S. Sariciftci, L. Smilowitz, A.J. Heeger, F. Wudl, *Science* 258 (1992) 1474.
- [4] J. Rostalski, *Der Photovoltaisch aktive Bereich molekularer organischer Solarzellen*, Ph.D. Thesis, Fachbereich 1, Rheinisch Westfälisch Technische Hochschule Aachen, 1999.
- [5] J. Rostalski, D. Meissner, *Sol. Energy Mater. Sol. Cells* 63 (2000) 37.
- [6] L.A.A. Petterson, L.S. Roman, O. Inganäs, *J. Appl. Phys.* 86 (1999) 487.
- [7] G. Meinhardt, D. Gruber, G. Jacopic, Y. Geerts, W. Papousek, G. Leising, *Synth. Met.* 121 (2001) 1593.
- [8] K.L. Eskenas, K.W. Mitchell, *Conference Record of the Eighteenth IEEE Photovoltaic Specialists Conference*, New York, 1985, p. 720.
- [9] L.A. Brickman, *Seventh E. C. Photovoltaic Solar Energy Conference Proceedings*, Dordrecht, 1987, p. 1050.
- [10] F. Leblanc, J. Perrin, J. Schmitt, *J. Appl. Phys.* 75 (1994) 1074.
- [11] G. Tao, J.W. Metselaar, *Proc. SPIE* 2531 (1995) 185;
M. Zeman, R.A.C.M.M. van Swaaij, J.W. Metselaar, R.E.I. Schropp, *J. Appl. Phys.* 88 (2000) 6436;
M. Zeman, R.A.C.M.M. van Swaaij, M. Zuideam, J.W. Metselaar, R.E.I. Schropp, *Sol. Energy Mater. Sol. Cells* 66 (2001) 353.

- [12] M.Y. Ghannam, A.A. Abouelsaood, R.P. Mertens, *J. Appl. Phys.* 84 (1998) 496.
- [13] B. Sopori, J. Madjdpour, Yi-Zhang, Wei-Chen, PV optics: an optical modeling tool for solar cell and module design, *Electrochemical Society Proceedings*, Vols. 99–11, Pennington, NJ, 1999, p. 138.
- [14] R. Brendel, D. Scholten, *Appl. Phys. A* 69 (1999) 201.
- [15] S.F. Rowlands, J. Livingstone, C.P. Lund, *Sol. Energy Mater. Sol. Cells* 71 (2002) 399.
- [16] A. Usami, *Sol. Energy Mater. Sol. Cells* 64 (2000) 73.
- [17] M. Niggemann, B. Bläsi, A. Gombert, A. Hinsch, H. Hoppe, P. Lalanne, D. Meissner, V. Wittwer, Trapping light in organic plastic solar cells with integrated diffraction gratings, *Proceedings of the 17th European Photovoltaic Solar Energy Conference*, Munich, Germany, 2001.
- [18] B. Harbecke, *Appl. Phys. B* 39 (3) (1986) 165.
- [19] O.S. Heavens, *Optical Properties of Thin Solid Films*, Dover Publications, New York, 1991.
- [20] Sh.A. Furman, A.V. Tikhonravov, *Basics of Optics of Multilayer Systems*, Frontiers, Paris, 1996.
- [21] C.C. Kim, J.W. Garland, H. Abad, P.M. Racciah, *Phys. Rev. B* 45 (20) (1992) 11749.
- [22] L.D. Landau, E.M. Lifshitz, L.P. Pitaevskii, *Electrodynamics of Continuous Media*, 2nd Edition, Pergamon Press, Oxford, 1984, p. 80;
D. Bäuerle, *Laser Processing Chemistry*, 3rd Edition, Springer, Berlin, 2000, ch. 2.2.1.
- [23] B.E.A. Saleh, M.C. Teich, *Fundamentals of Photonics*, Wiley, New York, 1991, ch. 10.1.B.
- [24] H. Hoppe, N.S. Sariciftci, D. Meissner, *Mol. Cryst. Liquid Cryst.* 385 (2002) 113.